Earth-to-Halo Transfers in the Sun–Earth–Moon Scenario [⋆]

Anna Zanzottera [∗] **Giorgio Mingotti** [∗] **Roberto Castelli** [∗]
Michael Dellnitz [∗]

[∗] *IFIM, Universität Paderborn, Warburger Str. 100, 33098 Paderborn,*
Germany (e-mail: {annazanz,mingotti,robertoc,dellnitz} @math.upb.de)

Abstract: Trajectories connecting LEOs with halos around libration points of the Earth–Moon CRTBP are presented. Exploiting the coupled circular restricted three-body problem approximation suitable first guess trajectories are derived detecting intersections between stable manifolds related to halo orbits of EM spatial CRTBP and Earth-escaping trajectories integrated in planar SE CRTBP. The accuracy of the intersections in configuration space and the discontinuities in terms of Δv are controlled through the box covering structure implemented in the software GAIO. Finally first guess solutions are optimized in the bicircular four-body problem and single-impulse and two-impulse transfers are presented.

Keywords: Three-body problems; Halo orbits; Invariant manifolds; Box covering; Bicircular model; Trajectory optimization.

1. INTRODUCTION

This work deals with the design of trajectories connecting LEOs (low Earth orbits) with halo orbits around libration points of the Earth–Moon CRTBP, Szebehely (1967), using impulsive manoeuvres. The interest for such transfers comes mainly from the importance of halo orbits as possible location for lunar far-side data relay satellites; in particular a satellite evolving on a halo orbit will always maintain line of sight contact with the Earth and Moon's far side, Farquhar (1969).

Indeed,it is taken into account a $h_E = 167\,\mathrm{km}$ altitude parking orbit and a family of halo orbits associated to $L2$ Lagrangian point. As widely used in literature, suitable first guess trajectories are derived exploiting the *coupled circular restricted three-body problem approximation*, Belbruno and Miller (1993); Koon et al. (2001). This method consists in the superposition of two different CRTBPs, namely the SE (Sun–Earth) and EM (Earth–Moon) restricted problems. The transfer trajectories are obtained patching together on convenient Poincaré sections the invariant manifolds related to periodic orbits of the two systems. Such transfers are achieved if the Poincaré maps of the two problems intersect almost exactly in the configuration space.

In the current case, intersections between the stable manifolds - related to EM halo orbits - and Earth escape trajectories - integrated in the planar SE CRTBP - have to be detected. This is done using the software package GAIO: n-dimensional Poincaré maps are replaced by a collection of n-dimensional *boxes*, each one identified by a vector containing its center and the radii in each dimensions. The implemented box covering structure allows to deal with flows of different dimensions in an efficient way. Moreover,

the accuracy of the intersections in the configuration space, as well as the discontinuities in terms of Δv, are controlled through the parameters of the box covering. This exploration is systematically performed combining various halo orbits and Earth-escaping trajectories, with a choice of different Poincaré sections.

Then, first guess solutions are optimized through a direct method approach and multiple shooting technique, Betts (1998), in the framework of the Sun-perturbed Earth–Moon bicircular four-body problem, Simó et al. (1995). Finally, trajectories with single-impulse and two-impulse manoeuvres are presented and compared with results already known in literature, Parker (2006).

2. DYNAMICAL MODELS

In this section we present the dynamical system we will use to study the motion of a spacecraft in a field of three massive bodies.

2.1 Circular Restricted Three-Body Problem

The circular restricted three-body problem (CRTBP), Szebehely (1967), studies the motion of a massless particle P moving in the gravitational field of two main primaries, with masses $m_1 > m_2$. The primaries are supposed to move under their mutual gravity in circular orbits around the center of mass and their motion is not affected by the third particle. In this paper P represents the spacecraft while the role of primaries is played by Sun and Earth (SE CRTBP) or by Earth and Moon (EM CRTBP).

In a rotating reference frame where the units of measure are normalized so that the distance between the primaries, the modulus of their angular velocity and the total mass are equal to 1, the motion for the third body is governed by the equation

$$\begin{cases} \ddot{x} - 2\dot{y} = \Omega_x \\ \ddot{y} + 2\dot{x} = \Omega_y \\ \ddot{z} = \Omega_z \end{cases} \qquad (1)$$

where $\Omega(x,y,z) = \frac{1}{2}(x^2+y^2) + \frac{1-\mu}{r_1} + \frac{\mu}{r_2} + \frac{1}{2}\mu(1-\mu)$ is the effective potential of the system and the subscripts denote partial derivatives. Here $\mu = m_2/(m_1+m_2)$ is the mass ratio, while $r_1^2 = (x+\mu)^2+y^2+z^2$ and $r_2^2 = (x-1+\mu)^2+y^2$ are the distance from the spacecraft respectively to the larger and the smaller primary. The system (1) has a first integral of motion, the Jacobi integral, defined as:

$$C(x,y,z,\dot{x},\dot{y},\dot{z}) = 2\Omega(x,y,z) - (\dot{x}^2+\dot{y}^2+\dot{z}^2) \qquad (2)$$

As C^* varies, the family of 5-dimensional energy manifolds

$$\mathcal{M}(C^*) = \{(x,y,z,\dot{x},\dot{y},\dot{z}) : C(x,y,z,\dot{x},\dot{y},\dot{z}) = C^*\}$$

is a foliation of the 6-dimensional phase space. For every C^* the solution in the configuration space of the equation $C^* = 2\Omega(x,y,z)$ detects the zero-velocity surface, which bounds the Hill's region where the motion is possible and where it is forbidden.

The system (1) admits five equilibrium points, referred to as Lagrange points and denoted with Li, $i : 1 \ldots 5$: three of them $L1$, $L2$, $L3$ lie on the x-axis and represent collinear configurations, while $L4$, $L5$ correspond to equilateral configurations.

The topology of the Hill's region changes in correspondence to the values C_i of the Jacobi constant relative to the libration points, allowing to open necks between different regions on the configuration space.

The collinear libration points, as well as the continuous families of planar and spatial periodic orbits surrounding them, have a saddle-center type stability character: the invariant manifold related to these orbits act as separatrices in the energy manifold and provide dynamical channels in the phase space useful for design low cost spacecraft trajectories.

In this work the planar SE CRTBP and the spatial EM CRTBP are combined to the purpose of design initial guesses trajectories connecting a low Earth orbit with an halo orbit around $L2$ in the EM system.

2.2 Bicircular Restricted Four-Body Problem

The bicircular four-body model (BCRFBP) is a restricted four-body problem where two of the primaries (the Earth and the Moon) are moving in circular orbit around their center of mass B that is at the same time orbiting, together with the last mass (the Sun), around the barycenter of all the system. The motion of the primaries are supposed to be co-planar and with constant angular velocity. The equations of motion of the BCRFBP are written in the EM synodical reference frame and the physical quantities are normalized as in the EM CRTBP. Let m_s be the Sun mass, R_s the distance between the Sun and the origin of the frame B and ω_s the angular velocity of the Sun. Moreover let $\theta(t) = \theta_0 - \omega_s t$ the angle between the Earth–Moon line and the Sun, and r_s the Sun-spacecraft distance:

$$r_s^2 = (x - R_s\cos\theta)^2 + (y - R_s\sin\theta)^2 + z^2. \qquad (3)$$

The motion of the massless particle solves the system of differential equations

$$\begin{cases} \ddot{x} - 2\dot{y} = \Omega_{Bx} \\ \ddot{y} + 2\dot{x} = \Omega_{By} \\ \ddot{z} = \Omega_{Bz} \end{cases} \qquad (4)$$

where $\Omega_B = \Omega + \frac{m_s}{r_s} - \frac{m_s}{R_s^2}(x\cos\theta + y\sin\theta)$. In literature it is common to refer to the dynamical system (4) as the Sun–Perturbed Earth–Moon Bicircular Restricted Three-Body problem, Simó et al. (1995). Nevertheless, the bicircular model is not coherent because the motion of the primaries does not solve the three-body problem.
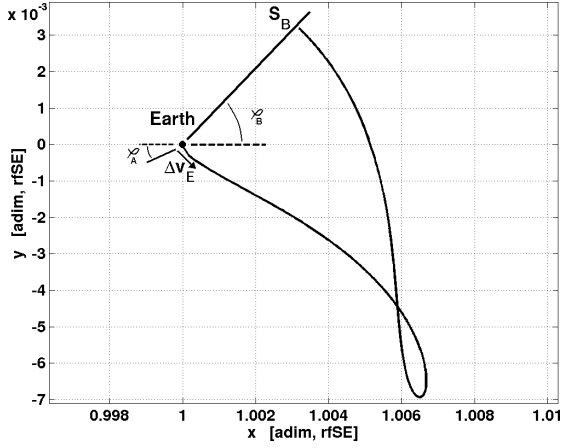
3. TRAJECTORY DESIGN

The aim of this paper is to find trajectories in the bicircular model, starting from a LEO and targeting a halo orbit around $L2$ in the EM restricted problem. Since the phase space of the four-body system is poor of useful dynamical properties, like equilibrium points or invariant manifolds, the design is first performed in the CRTBP and then the initial guess trajectories are optimized to be solution of the bicircular model.

The model adopted as approximation of the Sun-Earth-Moon-spacecraft restricted four-body problem is the so called Patched Restricted Three-Body Problem. It consists in the superposition of two CRTBPs with a common primary, namely the Sun–Earth CRTBP and the Earth–Moon CRTBP. The structure of the invariant manifolds associated to periodic orbits around the collinear libration points provides natural transfers from and to the smaller primaries. Then, by means of a Poincaré section the two legs of the trajectory are joined together, eventually with an impulsive manoeuvre, yielding a low energy ballistic transfer.

According to this procedure, the design of LEO-to-halo trajectories is conceived in two different stages: the *Earth escape stage* and the *halo capture stage*. In the first part the planar SE CRTBP is exploited to leave a LEO orbit of $h_E = 167$ km of altitude, then the invariant manifold of the three-dimensional EM CRTBP is followed to obtain a natural transfer to halo orbits. The Poincaré section is chosen as a hyperplane in the phase space passing through the Earth and perpendicular to the (x,y) plane. Its inclinations with respect to the positive x-semiaxis in the SE and EM synodical reference frame are denoted respectively with φ_B and φ_C and represent two of the free design parameters.

3.1 Earth Escape Stage

As above mentioned, the departure leg of the transfer consists in a trajectory leaving a LEO orbit and integrated in planar SE CRTBP until the section $S(\varphi_B)$ is reached. The launch point $\mathbf{y}_E(\varphi_A, \Delta v_E)$ is identified by the angle φ_A that the position on LEO forms with the Sun-Earth line and by the Δv_E manoeuvre applied to insert the spacecraft into the translunar trajectory (see Fig. 1(a)). The manoeuvre is chosen tangential with magnitude in the range $I = [3200, 3285]$ m/s. The choice of the interval I follows from the fact that the Jacobi constant associated to the spacecraft, in the SE coordinates system, needs to be decreased from the value related to a LEO orbit, $C_{SE} \approx 3.07053$, to a value just below C_2, that has been shown to reveal good opportunities for the design.

(a) Earth escape trajectory.
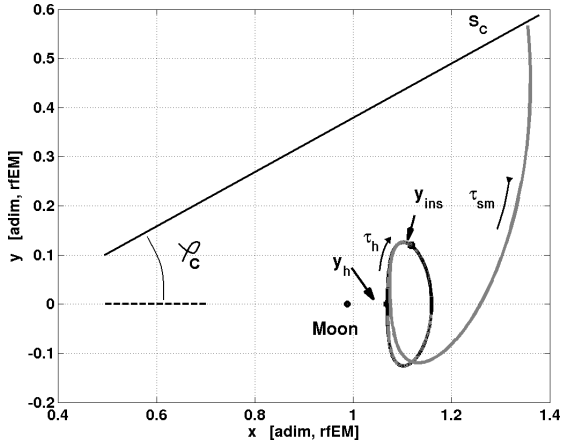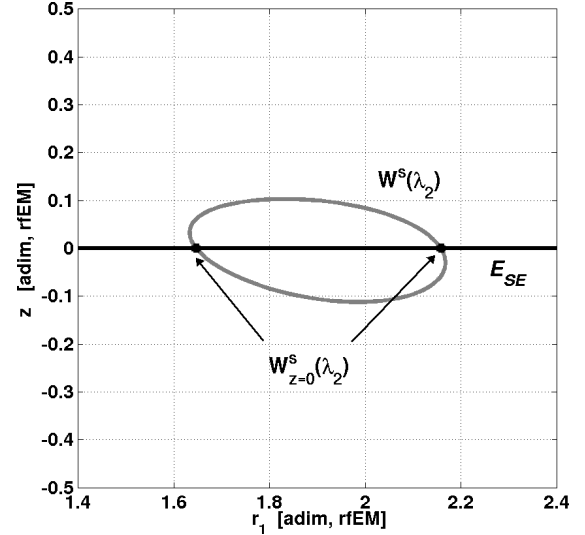

(b) Halo arrival trajectory.

Fig. 1. The two stages of the Earth-to-halo trajectory design.

(a) $E_{SE} \cap W^s(\lambda_2)$ in the r_1, z coordinates.

(b) $E_{SE} \cap W^s(\lambda_2)$ in the $r_1, \dot{r}_1$ coordinates.

Fig. 2. Transfer point definition on suitable Poincar'e maps.

For a set of 2000 value of $\varphi_A \in [0, 2\pi]$ and every integer value of $\Delta v_E \in I$, the initial state $\mathbf{y}_E(\varphi_A, \Delta v_E)$ is forward integrated in the SE CRTBP at most for one unit of time. For a value of the angle φ_B, let P_{SE} be the set of all the intersections that such paths have with the section $S_B(\varphi_B)$.
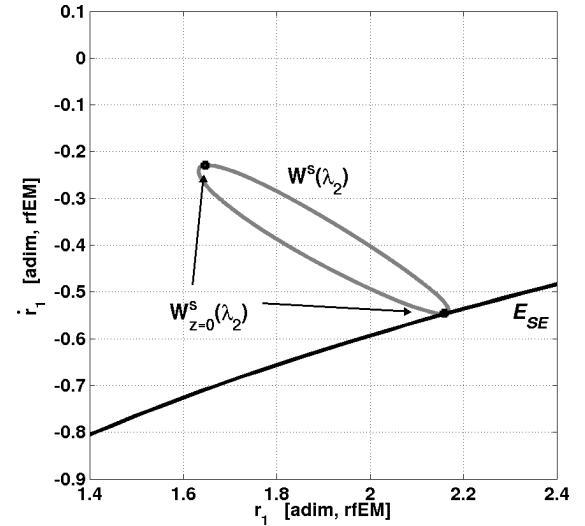
3.2 Halo Capture Stage

The second phase of the design exploits the (exterior) stable branch of the EM manifold related to a target halo orbit λ_2 around $L2$. The stable manifold $W^s(\lambda_2)$ is integrated backwards starting from λ_2 until the surface $S_C(\varphi_C)$ is reached: let P_{EM} the associated Poincaré map.

The halo orbit is identified by the nominal point $\mathbf{y}_h$ where the plane $\{y = 0\}$ is intersected with positive $\dot{y}$, while the state $\mathbf{y}(t)$ of a generic point on the stable manifold is unequivocally determined by two time parameters (τ_h, τ_{sm}). Denoting the insertion point $\mathbf{y}_{ins} = \phi(\mathbf{y}_h, 0; \tau_h)$, obtained by means of a forward integration (i.e. assuming $\tau_h \geq 0$), a generic point on the stable manifold reads $\mathbf{y}_{sm} = \phi(\tilde{\mathbf{y}}_{ins}, 0; \tau_{sm})$ (see Fig. 1(b)). Assuming $\tau_{sm} \leq 0$, a backward integration is taken into account starting from $\tilde{\mathbf{y}}_{ins}$, which stands for the ε-shift of $\mathbf{y}_{ins}$ along the stable direction provided by the monodromy matrix.

3.3 Box Covering Technique

Changing the parameters φ_B, φ_C, Δv_E, φ_A, $\mathbf{y}_{ins}$, the design of the trajectory is restricted to the detection on the Poincaré section of two points, $\mathbf{y}_B \in P_{SE}$ and $\mathbf{y}_C \in P_{EM}$. First the map P_{SE} is transformed in EM synodical coordinate system, being $\beta = \varphi_B - \varphi_C$ the angle between the Moon and the Sun-Earth line. Then, in order to obtain a feasible transfer, the pairs of points $\mathbf{y}_B$ and $\mathbf{y}_C$ which match almost exactly in configuration space are selected. Moreover, they are chosen to minimize as much as possible the distance in velocity space. If it is possible to achieve satisfying intersections in configuration space between P_{SE} and the subset $P_{EM} \cap \{|z| < \varepsilon\}$, the out-of-plane components of the velocity of the two points are always different. This is due because points belonging to P_{SE} are planar, while those belonging to P_{EM} are spatial.

The search of candidate transfer points is performed using a *box covering* structure implemented in the software package GAIO (Global Analysis of Invariant Objects), see Dellnitz and Junge (2002) for a detailed description.

An n-dimensional box $\mathcal{B}(C,R)$, identified by a center $C = (C_1, \cdots, C_N) \in \mathcal{R}^N$ and a vector of radii $R = (r_1, \cdots, r_n) \in \mathcal{R}^N$, is defined as

$$\mathcal{B}(C,R) = \cap_{i=1}^N \{(x_1, x_2, ...x_N) \in R^N : |x_i - C_i| < r_i\}$$

Starting from an initial box $\mathcal{B}_0$ containing the projection of P_{EM} on the configuration space, a multiple subdivision process is carried out to create families $\mathcal{F}_k$ of smaller boxes $\{\mathcal{B}_k\}$ with the property to cover $\mathcal{B}_0$, i.e. $\bigcup \mathcal{B}_k = \mathcal{B}_0$. In the k-th subdivision step each rectangle $\mathcal{B}(C,R)$ of the existing collection is subdivided with respect to the j-th coordinate, where j can vary cyclically or can be chosen by the user. Once the radii of the boxes in $\mathcal{F}_k$ reach a prescribed size $\bar{\sigma}$, the Poincaré map is inserted: only those boxes $\mathcal{B}_k$ with non empty intersection with P_{EM} are stored, otherwise removed. Denoting with $\mathcal{F}$ the collection of the remaining boxes, the feasibility condition previously discussed is fulfilled choosing the possible transfer points B in the intersection $\mathcal{F} \cap P_{SE}$. Clearly, since the P_{SE} lies on the $\{z = 0\}$ plane, only two boxes of $\mathcal{F}$ can satisfy this relation.

In the numerical simulation here presented, the Poincaré maps are at first transformed in EM cylindrical coordinates $(r_1, \theta, z, \dot{r}_1, r_1\dot{\theta}, \dot{z})$ centered in the Earth, then inserted into a collection of boxes with radii $\bar{\sigma}$, at most equal to 10^{-4} in r_1 and z coordinates. In Fig. 2(a), the intersection - in the space of configurations - of the Earth escape trajectories (E_{SE} black line) and the stable manifold related to the final halo target (grey curves $W^s(\lambda_2)$, for different φ_C) are shown. The black dots stand for the intersection of E_{SE} with the $\{z = 0\}$ plane. According to Fig. 2(b), it is possible to detect the candidate transfer points as the ones corresponding to $E_{SE} \cap W^s(\lambda_2)$.

4. TRAJECTORY OPTIMIZATION

This section gives firstly a brief introduction of the trajectory optimization approach used in this work, then formulates in details the minimization problems later solved.

Once feasible and efficient first guess solutions are achieved, combining the two legs of the transfer, an optimization problem is stated. A given objective function is minimized taking into account the dynamic of the process.
The dynamical model used to consider the gravitational attractions of all the celestial bodies involved in the design process (i.e. the Sun, the Earth, and the Moon) is the spatial BCRFBP described by (4) (written in an autonomous fashion) with the adding of the acceleration term:

$$\begin{cases} \ddot{x} - 2\dot{y} = \Omega_{Bx} \\ \ddot{y} + 2\dot{x} = \Omega_{By} \\ \ddot{z} = \Omega_{Bz} \\ \dot{\theta} = \omega_s \end{cases} \qquad (5)$$

According to the formalism proposed by Betts (1998), the BCRFBP described by (5) is written in the first-order form

$$\begin{aligned} \dot{x} &= v_x \\ \dot{y} &= v_y \\ \dot{z} &= v_z \\ \dot{v}_x &= 2v_y + \Omega_{Bx} \\ \dot{v}_y &= -2v_x + \Omega_{By} \\ \dot{v}_z &= \Omega_{Bz} \\ \dot{\theta} &= \omega_s \end{aligned} \qquad (6)$$
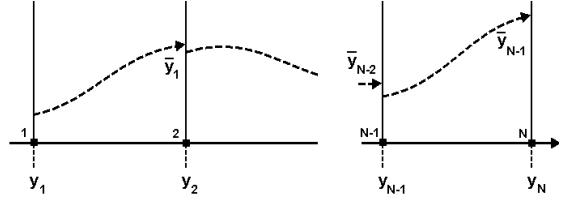

Fig. 3. Direct multiple shooting scheme.

with $v_x = \dot{x}$, $v_y = \dot{y}$ and $v_z = \dot{z}$. In a compact explicit form, system (6) reads

$$\dot{\mathbf{y}} = \mathbf{f}[\mathbf{y}(t), \mathbf{p}, t], \qquad (7)$$

where $\mathbf{f}$ stands for the vector field and the state vector is $\mathbf{y} = \{x, y, z, \dot{x}, \dot{y}, \dot{z}, \theta\}^\top$. The aim is finding $\mathbf{y} = \mathbf{y}(t)$, $t \in [t_i, t_f]$, that minimizes a prescribed scalar performance index or objective function

$$J = J(\mathbf{y}, \mathbf{p}, t), \qquad (8)$$

while satisfying certain mission constraints. These constraints are represented by the two boundary conditions, defined at the end points of the optimization problem, and by the inequality conditions, defined along the whole arc. These last quantities are derived specifically for the mission investigated. Moreover, $\mathbf{p}$ stands for a vector which brings together some free parameters useful for the optimization process.

The optimization problem, OP, is then transcribed into a nonlinear programming, NLP, problem using a direct approach. This method, although suboptimal, generally shows robustness and versatility, and does not require explicit derivation of the necessary conditions of optimality. Moreover, direct approaches offer higher computational efficiency and are less sensitive to variation of the first guess solutions, Betts (1998). Furthermore, a multiple shooting scheme is implemented. With this strategy the BCRFBP dynamics presented by (5) is forward integrated within $N-1$ intervals (in which $[t_i, t_f]$ is uniformly split), i.e. the time domain is divided in the form $t_i = t_1 < \cdots < t_N = t_f$, and the solution is discretized over the N grid nodes (see Fig. 3). The continuity of position and velocity is imposed at their ends, Enright and Conway (1992), in the form of defects $\boldsymbol{\eta}_j = \bar{\mathbf{y}}_j - \mathbf{y}_{j+1} = 0$, for $j = 1, \ldots, N - 1$. The quantity $\bar{\mathbf{y}}_j$ stands for the result of the integration, i.e. $\bar{\mathbf{y}}_j = \boldsymbol{\phi}(\mathbf{y}_j, \mathbf{p}, t)$, $t_j \leq t_{j+1}$. The algorithm computes the value of the states at mesh points, satisfying both boundary and path constraints, and minimizing the performance index.

Dynamics described by (5) are highly nonlinear and, in general, lead to chaotic orbits. In order to find accurate optimal solutions without excessively increasing the computational burden, an adaptive nonuniform time grid has been implemented. Thus, when the trajectory is close to either the Earth or the Moon the grid is automatically refined, whereas in the intermediate phase, where a weak vector field governs the motion of the spacecraft, a coarse grid is used. The optimal solution found is assessed a posteriori by forward integrating the optimal initial condition (with a Runge-Kutta 8th order scheme).

4.1 Two-Impulse Problem Statement

In this section, the approach previously described is exploited to obtain optimal transfers with two-impulsive manoeuvres.

According to the NLP formalism recalled, the variable vector is

$$\mathbf{x} = \{\mathbf{y}_1, \ldots, \mathbf{y}_N, t_1, t_N\}^\top. \qquad (9)$$

The initial conditions read:
$$\boldsymbol{\psi}_i(\mathbf{y}_1, t_1) :=$$
$$\begin{cases} (x_1 + \mu)^2 + y_1^2 + z_1^2 - r_i^2 = 0 \\ (x_1 + \mu)(\dot{x}_1 - y_1) + y_1(\dot{y}_1 + x_1 + \mu) + z_1\dot{z}_1 = 0, \end{cases}$$
$$(10)$$

which force the first $\mathbf{y}_1$ state of the transfer to belong to a circular orbit of radius $r_i = R_E + h_E$, where R_E and h_E stand for the Earth radius and the orbit altitude with respect to the Earth, respectively. The transfer ends when the spacecraft flies on the stable manifold related to the final halo. In details, only the continuity in terms of position is imposed, so that the final condition reads

$$\boldsymbol{\psi}_f = \overline{\mathbf{y}}_N - \overline{\mathbf{y}}_{sm} = 0, \qquad (11)$$

where it is worth noting that $\overline{\mathbf{y}}_N = \{x_N, y_N, z_N\}^\top$ and $\overline{\mathbf{y}}_{sm} = \{x_{sm}, y_{sm}, z_{sm}\}^\top$. This means that, after the initial impulsive maneuver, a second one is required to inject the spacecraft onto the stable manifold that takes it ballistically to the final halo orbit associated.

The nonlinear equality constraint vector, made up of the boundary conditions and the ones representing the dynamics, is therefore written as follows:

$$\mathbf{c}(\mathbf{x}) = \{\boldsymbol{\psi}_i, \boldsymbol{\eta}_1, \ldots, \boldsymbol{\eta}_{N-1}, \boldsymbol{\psi}_f\}^\top. \qquad (12)$$

Moreover, aiming at avoiding the collision with the two primaries, the following inequality constraints are imposed:

$$\boldsymbol{\Psi}_j^c(\mathbf{y}_j) := \begin{cases} R_E^2 - (x_j + \mu)^2 - y_j^2 - z_j^2 \leq 0 \\ R_M^2 - (x_j - 1 + \mu)^2 - y_j^2 - z_j^2 \leq 0, \end{cases} \qquad (13)$$
$$j = 2, \ldots, N - 1.$$

Finally, the flight time is searched to be positive, i.e.

$$\boldsymbol{\Psi}^t = t_1 - t_N \leq 0. \qquad (14)$$

The complete inequality constraint vector therefore reads:

$$\mathbf{g}(\mathbf{x}) = \{\boldsymbol{\Psi}_2^c, \ldots, \boldsymbol{\Psi}_{N-1}^c, \boldsymbol{\Psi}^t\}^\top. \qquad (15)$$

As for the performance index to minimize, this is a scalar that represents the two velocity variations at the beginning and at the final node of the transfer, i.e. $J(\mathbf{x}) = \Delta v_1 + \Delta v_N$. In details,

$$\Delta v_1 = \sqrt{(\dot{x}_1 - y_1)^2 + (\dot{y}_1 + x_1 + \mu)^2 + (z_1)^2} - v_i, \quad (16)$$

assuming $v_i = \sqrt{(1 - mu)/r_i}$ as the velocity along the initial circular parking orbit, and

$$\Delta v_N = \sqrt{(\dot{x}_N - \dot{x}_{sm})^2 + (\dot{y}_N - \dot{y}_{sm})^2 + (\dot{z}_N - \dot{z}_{sm})^2}, \qquad (17)$$

which represents the discontinuity in terms of velocity between the translunar trajectory and the stable manifold related to the final halo.

In summary, the NLP problem for the two-impulse transfers is formulated as follows:

$$\min_{\mathbf{x}} J(\mathbf{x}) \text{ subject to } \begin{array}{l} \mathbf{c}(\mathbf{x}) = 0, \\ \mathbf{g}(\mathbf{x}) \leq 0. \end{array} \qquad (18)$$

4.2 Single-Impulse Problem Statement

As for the single-impulse trajectories, the variable vector is stated as follows:

$$\mathbf{x} = \{\mathbf{y}_1, \ldots, \mathbf{y}_N, \mathbf{p}, t_1, t_N\}^\top, \qquad (19)$$

where $\mathbf{p} = \{\tau_h, \tau_{sm}\}$, which is made up of two free optimization parameters useful to describe the final condition of the transfer (see Fig. 1(b)).

The equality constraint vector is defined, as in the previous paragraph, by (12) with the exception of the final condition: in this case, at the final point of the transfer, the whole dynamical state is forced to be equal to the one associated to the stable manifold:

$$\boldsymbol{\psi}_f = \mathbf{y}_N - \mathbf{y}_{sm} = 0, \qquad (20)$$

where $\mathbf{y}_N = \{x_N, y_N, z_N, \dot{x}_N, \dot{y}_N, \dot{z}_N\}^\top$ and $\mathbf{y}_{sm} = \{x_{sm}, y_{sm}, z_{sm}, \dot{x}_{sm}, \dot{y}_{sm}, \dot{z}_{sm}\}^\top$.

In details, a generic point $\mathbf{y}_{sm}$ on the stable manifold is defined as described in section 3.2. Moreover, also the inequality constraint vector is defined in the same way as in the two-impulse scenario.

Dealing with the objective index to minimize, this is made up of only the initial velocity variation, i.e. the magnitude of the translunar insertion manoeuvre, i.e. $J(\mathbf{x}) = \Delta v_1$, where

$$\Delta v_1 = \sqrt{(\dot{x}_1 - y_1)^2 + (\dot{y}_1 + x_1 + \mu)^2 + (z_1)^2} - v_i. \quad (21)$$

Finally, the NLP problem for the low-energy low-thrust transfers is formulated as proposed by (18) at the end of the previous section.

5. OPTIMIZED TRANSFER SOLUTIONS

In this section the transfers to halos obtained solving the optimization process are presented. In the previous two sections, two families of trajectories are discussed, according to the number of impulsive manoeuvres that are allowed. In the following, the optimized solutions are proposed in terms of some relevant performance parameters.

5.1 Trajectories to Halos

Optimal two-impulse and single-impulse solutions are presented. These transfers start from a circular parking orbit at an altitude of $h_E = 167$ km around the Earth, and reach a halo orbit around $L2$, with an out-of-plane amplitude of $A_z = 8000$ km. The results are shown in table 1 as follows: the first sol.1 corresponds to the two-impulse low energy transfer, while solution sol.2 represents a single-impulse low energy transfer. Then, solutions below the line are some reference impulsive transfers found in literature.

More in details, Table 1 is so structured: the second column Δv_i stands for the initial impulsive manoeuvre that inserts the spacecraft onto the translunar trajectory. The third column Δv_f represents the final impulsive manoeuvre that permits the insertion of the spacecraft onto the stable manifold related to the target halo. For the solutions computed in this work, the value is present only for the two-impulse trajectories. The fourth column Δv_t represents the overall amount of impulsive manoeuvres

Table 1. Two-impulse and single-impulse low energy transfers to halos around $L2$. A set of impulsive reference solutions found in literature is also reported, (Parker (2006)).

Type	Δv_i [m/s]	Δv_f [m/s]	Δv_t [m/s]	Δt [days]
sol.1	3110	214	3324	98
sol.2	3161	0	3161	97
Parker.1	3132	618	3750	–
Parker.2	3235	0	3235	–
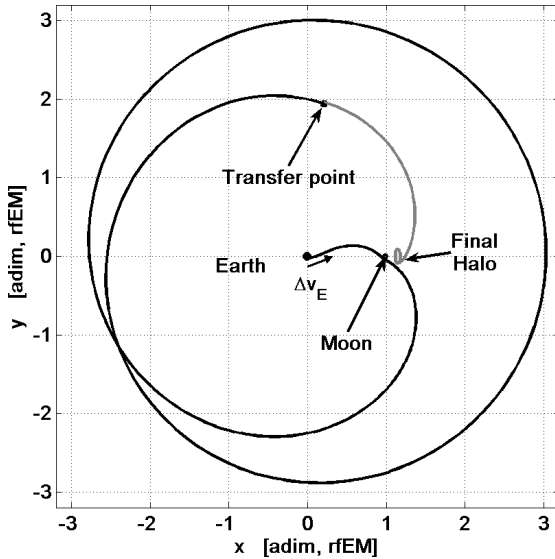
(a) First guess solution in Earth–Moon rotating frame.
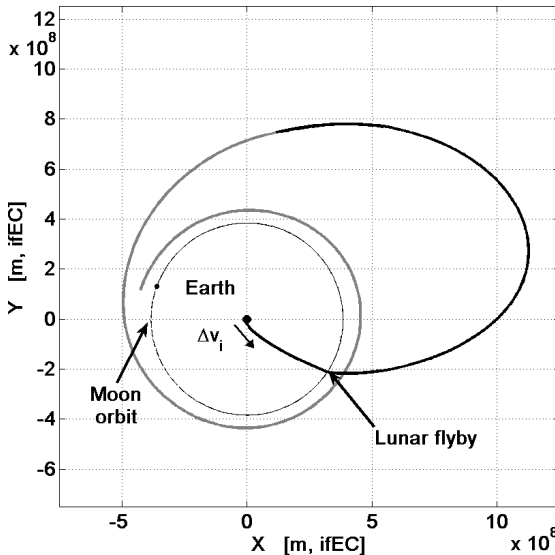
(b) Optimized trajectory in Earth centered inertial frame.

Fig. 4. First guess solution and optimized trajectory corresponding to sol.2 of table 1.

necessary to complete the Earth-to-halo transfers. Finally, the last column on the right stands for the transfer time.

An analysis of the table shows that the single-impulse sol.2 (see Fig. 4(a)) offers the lowest value of the overall impulsive manoeuvres (see Δv_t). This happens because the first guess solution exploits deeply the dynamics of the RTBPs where they are designed, and later of the Earth–Moon BRFBP where they are optimized. Moreover, this trajectory takes explicitly advantage of the initial lunar flyby. The latter can be seen as a kind of aid in the translunar orbit insertion, as it reduces the Δv_i required for that manoeuvre. The lunar flyby performs a change of plane of the translunar trajectory that allows the insertion of the spacecraft onto the three-dimensional halo stable manifold without any other manoeuvre. Summarizing, the single-impulse trajectory corresponding to sol.2 acknowledges these remarks, as it shows the lowest global $\Delta v_t = 3161\,\mathrm{m/s}$ (with travel time $\Delta t = 98\,\mathrm{days}$).

6. FINAL REMARKS

In this paper a technique to design two-impulse and single-impulse low energy transfers has been investigated. They revealed to be efficient, both in terms of Δv and flight time. The optimization approach resulted robust and versatile, and the obtained solutions have been *a posteriori* validated by means of a Runge-Kutta 8th order scheme. Moreover, through the box covering technique, an immediate definition of the transfer points in the phase space was possible, allowing to formalize a systematic method to intersect three-dimensional manifolds.

REFERENCES

E.A. Belbruno and J.K. Miller. Sun-Perturbed Earth-to-Moon Transfers with Ballistic Capture. *Journal of Guidance Control and Dynamics*, 16:770–775, 1993.

J.T. Betts. Survey of Numerical Methods for Trajectory Optimization. *Journal of Guidance control and dynamics*, 21(2):193–207, 1998.

M. Dellnitz and O. Junge. Set Oriented Numerical Methods for Dynamical Systems. *Handbook of dynamical systems*, 2(1):900, 2002.

P.J. Enright and B.A. Conway. Discrete Approximations to Optimal Trajectories Using Direct Transcription and Nonlinear Programming. *Journal of Guidance Control and Dynamics*, 15:994–1002, 1992.

R. Farquhar. Future Missions for Libration-Point Satellites. *Astronautics and Aeronautics*, 7:52–56, 1969.

W. Koon, M. Lo, J. Marsden, and S. Ross. Low Energy Transfer to the Moon. *Celestial Mechanics and Dynamical Astronomy*, 81:63–73, 2001.

J.S. Parker. Families of Low-Energy Lunar Halo Transfers. In *AAS/AIAA Spaceflight Dynamics Conference*, volume 90, pages 1–20, 2006.

C. Simó, G. Gómez, A. Jorba, and J. Masdemont. The Bicircular Model near the Triangular Libration Points of the RTBP. In *From Newton to Chaos*, pages 343–370, 1995.

V. Szebehely. *Theory of Orbits: the Restricted Problem of Three Bodies*. Academic Press New York, 1967.